HHS Public Access

Author manuscript

Acta Biomater. Author manuscript; available in PMC 2018 August 01.

Published in final edited form as:

Acta Biomater. 2017 August ; 58: 214–224. doi:10.1016/j.actbio.2017.05.057.

Simultaneous Delivery of Hydrophobic Small Molecules and siRNA Using Sterosomes to Direct Mesenchymal Stem Cell Differentiation for Bone Repair

Zhong-Kai Cui[a], **Justin A. Sun**[b], **Jessalyn J. Baljon**[b], **Jiabing Fan**[a], **Soyon Kim**[b], **Benjamin M. Wu**[a,b], **Tara Aghaloo**[c], and **Min Lee**[a,b,*]

[a]Division of Advanced Prosthodontics, University of California Los Angeles, 10833 Le Conte Avenue, Los Angeles, CA 90095, USA

[b]Department of Bioengineering, University of California Los Angeles, 420 Westwood Plaza, Los Angeles, CA 90095, USA

[c]Division of Diagnostic and Surgical Sciences, University of California Los Angeles, 10833 Le Conte Avenue, Los Angeles, CA 90095, USA

Abstract

The use of small molecular drugs with gene manipulation offers synergistic therapeutic efficacy by targeting multiple signaling pathways for combined treatment. Stimulation of mesenchymal stem cells (MSCs) with osteoinductive small molecule phenamil combined with suppression of noggin is a promising therapeutic strategy that increases bone morphogenetic protein (BMP) signaling and bone repair. Our cationic Sterosome formulated with stearylamine (SA) and cholesterol (Chol) is an attractive co-delivery system that not only forms stable complexes with small interfering RNA (siRNA) molecules but also solubilizes hydrophobic small molecules in a single vehicle, for directing stem cell differentiation. Herein, we demonstrate the ability of SA/Chol Sterosomes to simultaneously deliver hydrophobic small molecule phenamil and noggin-directed siRNA to enhance osteogenic differentiation of MSCs both in *in vitro* two- and three-dimensional settings as well as in a mouse calvarial defect model. These results suggest a novel liposomal platform to simultaneously deliver therapeutic genes and small molecules for combined therapy.

Graphical Abstract

* leemin@ucla.edu, Tel: +1 310-825-6674, Fax: +1 310-825-6345.

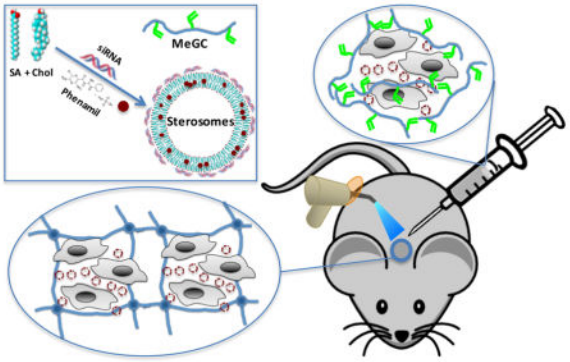

Keywords

co-delivery; Sterosomes; hydrophobic small molecular drugs; siRNA; osteogenic differentiation

1. Introduction

Dr. Alec Bangham et al. first reported their discovery of liposomes in 1964.[1] Over the past half century, liposomal nanotechnology has significantly advanced and provides medical and pharmaceutical benefits.[2, 3] Liposomes have already been commercialized for various therapies: Doxil®, Caelyx® and Myocet® are used to treat Kaposi's sarcoma, ovarian and metastatic breast cancer, multiple myeloma; and DaunoXome® for Kaposi's sarcoma. Visudyne® is used for age-related macular degeneration, myopia and ocular histoplasmosis; Ambisome® against fungal infection. DepoDur® is applied for pain relief following surgery. Combined treatment *via* simultaneous delivery of drugs and genetic materials in a single delivery vehicle presents potential advantages compared with individual therapy: synergistic effects of multiple medications,[4] suppressed drug resistance,[5] fine-tune of the dosages of multiple agents, etc. However, the natures of macromolecular nucleic acids and small molecular drugs are intrinsically different, presenting challenges in the development of co-delivery vehicles. Liposomes are essentially used as nanocarriers for protecting, transporting and targeting solutes. Liposomes can encapsulate both hydrophilic drugs in the aqueous core and hydrophobic drugs in the lipid bilayers. In gene therapy, cationic liposomes are reported to interact and complex with DNA, RNA or oligonucleotides, markedly prevent nuclease degradation, facilitate the intracellular uptake and further endosomal escape of oligonucleotide and result in a better intracellular distribution.[6–8] In light of these properties, liposomes are great candidates for co-delivery of small molecular drugs and nucleic acids. Recently, it has been reviewed that mixture of single-chain amphiphiles and high content sterols can form fluid lamellar phases. Even though these single-chain amphiphiles or sterols do not form fluid lamellar phases once hydrated individually, their mixtures lead to stable liquid-ordered bilayers, and the resulting liposomes were named Sterosomes because of the high sterol content.[9] Compared to the commercially available lipofectamine 2000, cationic Sterosomes formulated with stearylamine (SA) and cholesterol (Chol) showed significantly increased nanoparticle stability and cellular uptake efficiency in our previous study.

The use of mesenchymal stem cells (MSCs) is an attractive option to enhance bone tissue engineering.[10] However, MSCs alone had very limited success on bone repair in challenging healing environments.[11, 12] Bone morphogenetic protein-2 (BMP-2) is believed to be the most potent cytokine to promote osteogenic differentiation of MSCs and bone regeneration with extensive clinical use.[13, 14] Supraphysiologic BMP-2 dosage is, however, required for clinical treatment, leading to worrisome side effects including ectopic bone formation, life-threatening tissue swelling and cancer.[13, 15] Thus, recent promising alternative strategies are toward complementing BMP activity in MSC osteogenesis.

Phenamil, a small molecular derivative of diuretic amiloride, is found to promote BMP activity through upregulating tribbles homolog 3 (Trb3), a positive regulator of BMP signaling.[16] Phenamil enhanced osteogenesis and calvarial bone formation induced by BMP-2 while significantly lowering total BMP-2 dose.[17] The use of small molecules presents several advantages over growth factor therapies, including high stability, non-immunogenicity and relatively low cost. However, hydrophobic nature of such small molecules including phenamil requires the use of toxic organic solvents and often limits their clinical potential.[18, 19]

Upon BMP stimulation, BMP efficacy is greatly reduced due to the enhanced expression of natural BMP antagonists such as noggin to auto-regulate endogenous BMP-2 levels. Noggin is a secreted polypeptide that binds BMPs and inhibits their function by preventing BMP from binding their receptors on the cell surface. Small interfering RNA molecules have been used to downregulate expression of noggin, therefore to enhance osteogenesis *in vitro* as well as bone formation *in vivo*.[20–22] Our previous studies of viral mediated noggin knockdown showed that suppression of noggin enhanced both osteogenic differentiation of MSCs *in vitro*[23] and bone formation *in vivo* with both calvarial[24] and mandibular[25] defect models. However, delivery of noggin-directed RNAi molecules *via* non-viral modalities will be more advantageous by avoiding viral insertional mutagenesis.

In this work, we demonstrated the ability of the novel Sterosomes formulated with a single-chain amphiphile SA and high content of Chol to simultaneously deliver phenamil and noggin siRNA to enhance osteogenic differentiation of MSCs. Synergistic osteogenic effects were achieved by stimulating BMP signaling (phenamil) and simultaneously knocking down BMP antagonist noggin (siRNA) in a single vehicle. First, we evaluated the encapsulation and release of phenamil with SA/Chol vesicles, and assessed the bioactivity of the encapsulated phenamil compared with its free form dissolved in DMSO. We further investigated the ability of SA/Chol Sterosomes loaded with phenamil and noggin siRNA to induce osteogenic differentiation of MSCs in two-dimensional (2D) monolayer cell culture as well as in three-dimensional (3D) setting using hydrogels *in vitro*. Finally, the *in vivo* osteogenic ability of phenamil + noggin siRNA co-delivered with SA/Chol Sterosomes was evaluated in a mouse calvarial defect model. This present work demonstrated a novel and efficient co-delivery liposomal system containing small molecular drugs and nucleic acids in a single vehicle to guide stem cell differentiation, and this liposomal platform may provide new therapeutic biomaterial systems to improve current bone repair strategies.

2. Materials and methods

2.1. Materials

1-Aminooctadecane (SA, 99.0%), 3β-Hydroxy-5-cholestene (Chol, >99%), phenamil methanesulfonate salt (Phe), benzene (high purity), methanol (spectrograde), dimethyl sulfoxide (DMSO, >99%), tris(hydroxymethyl)-aminomethane (TRIS, 99%), NaCl (>99%), β-glycerophosphate, L-ascorbic acid, dexamethasone, Nitro Blue Tetrazolium (NBT), 5-Bromo-4-chloro-3-indolyl phosphate disodium salt (BCIP), p-nitrophenol phosphate, alkaline buffer solution, *p*-nitrophenylphosphate (pNPP), Alizarin Red S, ethylenediaminetetraacetic acid (EDTA) and Tween 20 were supplied by Millipore Sigma (St. Louis, MO). RNeasy Mini Kit was obtained from Qiagen (Valencia, CA). Trizol, SuperScript® III First-Strand Synthesis System, Dulbecco's Modified Eagle's Medium (DMEM, 1 g/L glucose), Penicillin/Streptomycin (100 U mL^{-1}, P/S) were obtained from Life Technologies (Grand Island, NY). Fetal Bovine Serum (FBS) was purchased from Mediatech Inc. (Manassas, VA). siRNA was provided by Santa Cruz Biotechnology (Santa Cruz, CA). All reagents were used as received. C57BL/6 and nude mice were ordered from Charles River Laboratories (Wilmington, MA).

2.2. Preparation of Sterosomes

First, dissolve stearylamine, cholesterol and phenamil proportionally in benzene/methanol (90/10 v/v). Freeze the above solutions in liquid nitrogen, and lyophilize them overnight to completely eliminate the organic solvent.[26] Then, Hydrate the freeze-dried mixtures in a pH 7.4 TRIS buffer (TRIS 50 mM, NaCl 140 mM). Carry out five cycles from liquid nitrogen temperature to ~70 °C, and vortex between successive cycles to obtain well-hydrated samples. Finally, liposomes were obtained with probe sonicator (20 s on and 5 s off) for 20 min.

A Sephadex G-50 spin column (diameter 0.4 cm, length 7 cm) was centrifuged at 3500 rpm for 1 min to separate free phenamil from phenamil-containing liposomes.[27] Phenamil and cholesterol content of the collected fraction were quantified using UV-Vis spectrometer and Cholesterol Fluorometric Assay Kit (Cayman Chemical, Ann Arbor, MI).

siRNA and Sterosomes complexation was prepared and validated according to our previous work.[24] Briefly, Sterosomes and siRNA were diluted separately in Tris-NaCl buffer in Eppendorf tubes and kept at room temperature for 5 min. The contents of two tubes were combined and incubated at room temperature for 20 min.

A Malvern Zetasizer was employed to determine the hydrodynamic diameters and the zeta potential of obtained Sterosomes at 25 °C.

2.3. Permeability of Encapsulated Phenamil in Sterosomes

The cumulative release of phenamil was assessed as a function of time by isolating the encapsulated phenamil of a 100-μL aliquot of the vesicle suspension using a Sephadex G-50 spin column. The phenamil concentration of the eluted fraction was quantified with a UV-

Vis spectrometer. The cholesterol content of the collected fraction was assayed with cholesterol fluorometric assay kit for normalization.

2.4. 2D Cell Culture

Adipose derived mesenchymal stem cells were obtained according to our previous protocol.[25, 28] All 2D cultures were carried out with 12-well plate in this work. The osteogenic medium (DMEM, 10% FBS, 1% P/S, 10 mM β-glycerophosphate, 50 μg mL^{-1} L-ascorbic acid, and 100 nM dexamethasone) was added in the wells once cells reached ~90% confluence. The cells were cultured with various nanoparticles in osteogenic medium.

2.5. Alkaline Phosphatase Staining and Quantification in 2D Culture

At day 3 and 7, cells were fixed in 10% formalin for 20 min, washed with PBS, and incubated in an NBT and BCIP solution in the ALP buffer (100 mM Tris, 50 mM $MgCl_2$, 100 mM NaCl, pH 8.5) for 2 h. The images of stained samples were taken on an Olympus IX71 microscope (Olympus, Tokyo, Japan). ALP expression was stained blue. ALP activity was quantified with the Alkaline phosphatase colorimetric assay. Briefly, cells were lysed with Tween 20 0.1% buffered in phosphate and collected from the 12-well plates, followed by 1 s sonication. Followed by 5 min centrifugation at 10000 rpm, the supernatant was used for the assay. The supernatant was pipetted to a 96-well plate and the reaction with phosphatase substrate remained for 2 h at room temperature. The plate was read at 405 nm to determine ALP concentration, which was normalized with the Micro BCA protein assay kit (Thermo Scientific, Rockford, IL).

2.6. RNA Extraction and qRT-PCR

Gene expression was quantified with 12-well plate 2D cultures of MSCs. The osteogenic medium with various nanoparticles was applied once cells reached ~80% confluence to induce cell differentiation. After incubation for 3 and 7 days in the osteogenic media, RNA was extracted using Trizol reagent and RNeasy Mini kit. 500 ng of extracted RNA was reversely transcribed to cDNA. Gene expression was quantified with a LightCycler 480 PCR (Indianapolis, IN) with 20 μL SYBR Green for 50 cycles. Fold changes in gene expression were calculated using the 2ˆ(−delta delta Ct) method. The relative gene expression level of interest was calculated compared to GAPDH, and then normalized to the expression induced in the control group. The sequences of the primers used in this experiment were as follows — *GAPDH*: AGGTCGGTGTGAACGGATTTG (forward), TGTAGACCATGTAGTTGAGGTCA (reverse); *Noggin*: GCCAGCACTATCTACACATCC (forward), GCGTCTCGTTCAGATCCTTCTC (reverse); *Alkaline phosphatase (ALP)*: GTTGCCAAGCTGGGAAGAACAC (forward), CCCACCCCGCTATTCCAAAC (reverse); *Runt-related transcription factor 2* (*Runx2*): CGGTCTCCTTCCAGGATGGT (forward), GCTTCCGTCAGCGTCAACA (reverse); *Osteocalcin (OCN)*: GGGAGACAACAGGGAGGAAAC (forward), CAGGCTTCCTGCCAGTACCT (reverse).

2.7. 3D Cell Culture

Preparation of MeGC was according to our previous protocol.[29] Mix 2×10^6 cells mL^{-1} and various nanoparticles (final concentration of 100 nM for siRNA) in MeGC solution

(final concentration of 2% w/v). 40 μL of the suspension gelled under visible blue-light (400 – 500 nm, 500 – 600 mW cm-^{2}, Bisco Inc., Schaumburg, IL) in the presence of a photoinitiator, riboflavin (final concentration 6 μM) for 40 s.

2.8. Cytotoxicity

AlamarBlue assay (Invitrogen, Carlsbad, CA) and Live/Dead staining were employed to evaluate cytotoxicity of nanoparticles in 3D settings. Briefly, MSCs encapsulated hydrogels with various concentrations of nanoparticles were incubated for 24 h in fresh basal growth medium, and then the medium was replaced with 10% (v/v) alamarBlue solution in basal growth medium. After 3 h incubation, the fluorescence intensity (F) of alamarBlue was read at 585 nm with an excitation wavelength of 570 nm. 100% viability was defined with the group of cells without nanoparticles. The blank group was set as a MeGC gel without cells incubated in the 10% (v/v) alamarBlue solution. The relative cell viability (%) was calculated using the following equation:

$$Relative\ cell\ viability = \frac{F_s - F_b}{F_c - F_b}, \quad (1)$$

where F_s, F_c, and F_b are fluorescence intensity of samples, control group, and blank group, respectively.

Live/Dead staining was performed using Live/Dead solutions from Invitrogen. Briefly, gels were washed with PBS and incubated in a Live/Dead solution at 37 °C for 15 min. The images of stained samples were captured on the Olympus IX71 microscope.

2.9. Alkaline Phosphatase and Alizarin Red S Staining and Quantification in 3D Settings

At a preset time-point, gels were fixed in 10% formalin for 20 min, washed with PBS, and incubated in an NBT and BCIP solution in the ALP buffer for 2 h. The images of stained samples were taken on an Olympus SZX16 Stereomicroscope (Olympus, Tokyo, Japan). ALP expression was stained blue. For ALP activity assay, gels were washed with PBS, incubated in 0.1% Tween 20 buffered in PBS at 4 °C for 5 min. ALP activity was quantified with the Alkaline phosphatase colorimetric assay and read at 405 nm, which was normalized to total DNA contents measured with the picogreen assay (Thermo Scientific, Rockford, IL).

Gels were fixed in 10% formalin for 20 min, washed with PBS, and incubated in 2% Alizarin red S solution for 5 min. Then, the gels were washed for 16 h in PBS (refreshed three times) to remove excess staining agent. The images of stained samples were captured on the Olympus SZX16 Stereomicroscope. Calcium deposition was stained red. The semiquantification of alizarin red staining was performed with calcium extraction in acetic acid and ammonium hydroxide neutralization, followed by colorimetric reading at 405 nm. [30]

2.10. Calvarial Defect Model

The surgical procedures strictly followed the guidelines of the Chancellor's Animal Research Committee at the University of California, Los Angeles. 3-mm full-thickness

calvarial defects were created on male CD-1 nude mice (8–12 weeks old) in the right side of parietal bone with a trephine drill. Each defect was injected with 10 μL MeGC hydrogels containing various nanoparticles and cells or left empty. After surgery, all animals were fully recovered and transferred to the vivarium. Water containing trimethoprim-sulfamethoxazole was provided for all animals to prevent potential infection for 7 days. More details can be found in our previous work.[24]

2.11. μCT Scanning and Analysis

Calvarial tissues of all experimental mice were extracted at week 6 for analysis. The harvested calvarial tissues were fixed in 4% formaldehyde at room temperature for 48 h, rinsed thoroughly with PBS and imaged with a high–resolution μCT (SkyScan 1172; SkyScan, Kontich, Belgium) with 57 kVp, 184 μA, 0.5 mm aluminum filtration and 10 μm resolution. CT images were viewed using OsiriX MD imaging software. New bone surface area was quantified with ImageJ software (NIH, Bethesda, Maryland).

2.12. Histological Evaluation

After CT scanning, the fixed tissues were immersed in 10% EDTA solution (refreshed once at day 3) under gentle shaking for 1 week. Decalcified samples were embedded in paraffin and cut into sections of 4 μm thickness. The tissue sections were deparaffinized and stained with hematoxyline and eosin (H&E) and Masson-Goldner trichrome (MGT). New or mature bone was stained green, and images were taken on the Olympus IX71 microscope. The diameter of the remaining defects was measured and normalized to the blank group to derive a percentage length change.

Immunohistochemistry was carried out on additional sections to stain noggin, Trb3 and OCN expression. The deparaffinized slides were treated with citric acid antigen retrieval, incubated with the primary antibodies noggin, Trb3 and OCN (Santa Cruz Biotechnology Inc., CA) and stained by HRP/DAB detection kit (Abcam, MA) as per instructions from manufacture.

2.13. Statistical Analysis

All experiments were performed independently at least three times, unless otherwise stated, and the values in all figures are average ± standard deviation. The analysis of variances (ANOVA) and Tukey's *post hoc* test were calculated with Origin 8.0 for statistical analysis and $p < 0.05$ was considered statistically significant.

3. Results and discussion

3.1. Characterization of Phenamil Loaded Sterosomes

Being a hydrophobic drug, entrapment of phenamil into lipid bilayers is the loading strategy employed in this study. The encapsulation efficiency of phenamil prepared with this method was 73.9±5.6% and a final drug-to-lipid ratio of 0.048±0.012 wt/wt was achieved. The hydrodynamic diameters of SA/Chol liposomes before and after phenamil encapsulation were around 129 and 126 nm, respectively and remained constant for at least 14 days, with a low (< 0.300) polydispersity distribution indices (PDI). After phenamil loading, no

significant changes in size were observed. The liposomal surface charge density can be readily investigated by microelectrophoresis and characterized by the zeta potential. The zeta potential of Sterosomes crafted from equimolar SA/Chol mixtures was 55 ± 2 mV at pH 7.4, indicating that the suspension is very stable.[31] The encapsulation of phenamil did not significantly change the zeta potential of Sterosomes (53 ± 2 mV), indiciating that phenamil was incorporated inside the bilayer without affecting the surface properties. The hydrodynamic diameter of phenamil-noggin siRNA loaded Sterosomes was measured to be 155 nm with a low PDI (<0.300) and zeta potential was 33 mV. Loading of siRNA into the phenamil-encapsulated Sterosomes had no significant effect on particle size but decreased the positive surface charge density as expected.

Release profile of phenamil from SA/Chol Sterosomes is shown in Figure 1. There was approximately 5% drug leakage after 24 h from Sterosomes, and loaded phenamil was slowly released in a sustainable manner up to 2 weeks. The observed sustained release can be attributed to the high Chol content in the liposomes making their bilayers more rigid and thicker, resulting in a limited permeability.[32] No obvious burst release was observed, indicating that phenamil-embedded Sterosomes are stable in suspension form. This feature is of importance and convenience for ready-to-use form and storage without premature drug release till further clinical use.

3.2. Bioactivity of Phenamil Loaded Sterosomes

MSCs in 2D monolayer culture were treated with various concentrations of phenamil in its free form (Phe) or encapsulated in SA/Chol liposomes (SA/Chol/Phe). The bioactivity of phenamil loaded in Sterosomes was evaluated by monitoring ALP expression in MSCs. The vesicle concentration was 5 μg mL^{-1}. Phenamil treatment increased the expression of ALP in MSCs at day 3 (Figure S1) and day 7 (Figure 2A) as the phenamil concentration increased from 1 to 20 μM The level of ALP expression in MSCs treated with free phenamil (5 μM) was comparable to that of MSCs treated with 10-fold less phenamil (500 nM) encapsulated in SA/Chol liposomes as quantified *via* colorimetric assay (Figure 2B). Simply after encapsulation with our Sterosomes, we have successfully reduced the dosage (at least 10-fold) of phenamil to achieve similar bioactivity compared to its free form solubilized in DMSO. Although the free-form phenamil was replenished at every medium change in 2D cultures, its osteogenic efficacy was significantly lower compared to the encapsulated form. It is possible that phenamil-loaded cationic Sterosomes are more interactive with cellular membrane, providing higher drug availability and rapid action. However, the results may not predict the most optimal phenamil dose and additional studies are needed to determine the dose-dependent effects of phenamil. The osteogenic activity of phenamil can be further enhanced by inhibiting expression of BMP antagonists such as noggin. The idea here is to explore the synergistic effects of phenamil and noggin siRNA *via* a single delivery vehicle on osteogensis. A scrambled siRNA construct was investigated to ensure the true effects of the noggin-specific siRNA in our previous work.[24] As expected, significantly enhanced ALP staining was observed for the co-delivery group comparing to single agent delivery with the same vehicle, indicating synergistic osteogenesis in 2D cultures.

3.3. Gene Expression

The expression of various osteogenic genes in MSCs was evaluated with qRT-PCR after co-delivery of phenamil and noggin siRNA within a single vehicle (Figure 3). More than 40% of noggin mRNA level was reduced by noggin siRNA delivered by SA/Chol vesicles compared to the groups without siRNA delivery. Co-encapsulation of phenamil did not significantly change the level of noggin knockdown, indicating that embedding phenamil in Sterosomes did not interfere with their gene knockdown efficiency. In addition, synergistic enhancement on osteogenic differentiation of MSCs in 2D cultures were further assessed by monitoring the gene expression of *ALP*, an early osteogenic marker, and *Runx2*, one of the most specific osteogenic differentiation markers in earlier stage and *OCN*, a late osteogenic marker (Figure 3). *ALP* expression was significantly higher in groups treated with 500 nM phenamil encapsulated in SA/Chol vesicles than groups treated with free phenamil at the same dosage and was comparable to groups treated with 20-fold more free phenamil (10 μM) on day 3. On day 7, *ALP* expression significantly elevated for phenamil and siRNA co-delivery group, ~1.5 fold change compared to groups with individual agent delivery or ~3 fold change compared to the control group. Significant upregulation of *Runx2* expression was observed for phenamil and siRNA co-delivery group, ~1.3 to ~2.5 fold changes compared to other groups. For the late marker *OCN* on day 7, significant elevation was observed for phenamil and siRNA co-delivery group. Taken altogether, simultaneous delivery of phenamil and noggin siRNA strongly enhanced osteogenic differentiation of MSCs with reduced dosage of small molecular drug. The synergistic effects of small molecular drugs and siRNA were simply achieved by co-encapsulating them into a single delivery vehicle. Further work on gene expression profiling for a longer period of time will elucidate the molecular mechanisms involved in co-delivery osteogenesis.

3.4. In Vitro Bioactivity in 3D Model

Positive charge of cationic liposomes can lead to the generation of reactive oxygen intermediates, toxic oxidative bursts, and a disruption of cellular and sub-cellular membrane functions.[33–35] Negatively charged siRNA can lower the cytotoxicity after complexation with cationic Sterosomes, due to partially neutralization of the positive charges. Since no cytotoxicity was observed in 2D monolayer cultures with SA/Chol nanoparticles in our previous study,[24] we further tested the nanoparticle cytotoxicity in 3D environments to better mimic *in vivo* cellular behaviors. We employed photocrosslinkable methacrylated glycol chitosan (MeGC) hydrogels[29]. Distinct characteristics of *in situ* forming 3D hydrogels promote their applications for tissue engineering, including their compositional and structural similarities to natural extracellular matrix, their injectability and capacity to gel to fill any irregular defect shapes and the capacity to encapsulate cells with high viability.[36, 37] The MeGC hydrogel system facilitated proliferation and osteo- or chondrogenic differentiation of encapsulated MSCs.[29, 38, 39] We evaluated the cytotoxic effects of SA/Chol Sterosomes by encapsulating them in the MeGC hydrogel with MSCs as described in our previous study.[29] Minimal cell death was observed up to 100 μg mL^{-1} as assessed by Alamar blue assay and Live/Dead staining (Figure S2).

We further evaluated the osteogenic differentiation of MSCs in the MeGC hydrogel containing SA/Chol Sterosomes. ALP expression and calcium deposition were examined *via*

ALP and Alizarin Red S staining and colorimetric quantification. A blank gel without cells served as a negative control, whereas all the other experimental groups contained MSCs. The intensity of ALP and calcium staining increased over time for all groups cultured in osteogenic media. The observed increase in background staining over time can be attributed to increased non-specific binding of serum proteins to a gel surface with a longer incubation time, resulting in darker background staining. We also evaluated phenamil release after encapsulating the phenamil-loaded Sterosomes in MeGC hydrogel and the hydrogel polymerization had no significant effect on the release profile (Figure S3). Our previous studies demonstrated that the bioactivity of growth factor proteins was well preserved during the photopolymerization process in MeGC gels.[40, 41] We would not expect negative effects of the irradiation process on the bioactivity of phenamil and siRNA in our experimental setting.

In Figure 4(A and B), the strongest ALP expression was observed for phenamil and siRNA co-delivered by SA/Chol vesicles for both day 3 and 7. ALP can also be produced by other cell phenotypes; hence it is essential to evaluate more specific osteogenic differentiation indicators as well. Mineralization is well known to be the ultimate indicator of osteogenic differentiation; the calcium deposition was examined by Alizarin red S staining. Figure 4(A and C) revealed increased extracellular matrix mineralization. Encapsulated phenamil (500 nM) has increased ALP expression and calcium deposition to a similar or greater extent than 10 μM free drug dissolved in DMSO consistent with 2D findings. Since many negative effects of hydrophobic drugs are dose-related, drug delivery *via* nanocarriers can decrease total dose requirements, thereby further enhancing efficiency and potentially efficacy. Simultaneous delivery of phenamil and noggin siRNA *via* SA/Chol Sterosomes considerably amplified their effects on osteogenic differentiation of MSCs compared to vehicles loaded with phenamil or noggin siRNA alone. We believe that this is a powerful approach for directing stem cell behaviors. Although we conducted the *in vitro* studies in routinely used osteogenic medium containing dexamethasone, dexamethasone is known to affect MSC osteogenic commitment and it would be interesting to evaluate nanocarrier efficacy without dexamethasone for the future clinical translation.

3.5. In Vivo Calvarial Defect Model

We took a further step with mouse calvarial defects model to evaluate the *in vivo* bone repair six weeks post-surgery (n = 4). Four groups with the same critical size (3 mm) defects were designed. The blank group was left empty without any treatment after creating the defect. All the other groups were treated with *in situ* forming MeGC hydrogels encapsulating MSCs and various nanocarriers. Our previous work showed that 100 μM phenamil was a minimal effective dose to induce bone repair in the calvarial defect.[17] Since we were able to decrease phenamil dose requirements 10–20 fold by phenamil encapsulation, we have chosen to deliver 5 μM encapsulated phenamil in 50 μg mL^{-1} SA/Chol nanoparticles for the *in vivo* settings. The size of the defects treated with MSCs and nanocarriers were significantly smaller than the blank control group. The most bone healing was observed with the phenamil and noggin siRNA co-delivery group (Figure 5A). The relative new bone surface area was calculated and normalized to the original defect area (d = 3 mm) to quantitatively analyze the μCT images (Figure 5B). Defects treated with phenamil, noggin

siRNA and their combination delivered by SA/Chol vesicles were filled ~36%, ~27% and ~52% by new bone, respectively. In contrast, blank defects showed a minimal healing (~10%) after 6 weeks.

Histological analysis (Figure 6A) was carried out to further analyze the new bone formation. H&E staining showed that the edges of defects treated with nanoparticles were filled with bone tissue 6-week post-surgery. Masson-Goldner trichrome staining showed formation of osteoid matrix on the edges of defects, while the blank group only displayed fibrous-like tissue with minimal bone formation. The diameter of the remaining defects was smaller for groups treated with agent-loaded nanocarriers compared to the blank group. The relative length change was measured with ImageJ and presented in Figure 6B. For phenamil, noggin siRNA and their combination delivered by SA/Chol vesicles, the diameter of the remaining defects decreased by ~28%, ~26% and ~45% compared to the blank group, respectively. The edges of the advancing bone are indicated by red vertical lines as shown in Figure 6A. Furthermore, we evaluated expression of noggin, Trb3 and OCN 6-week post-implantation by immunohistochemical staining (Figure 7). Noggin staining was reduced in the SA/Chol/nogRNA and SA/Chol/Phe+nogRNA groups compared to the blank and SA/Chol/Phe groups, suggesting noggin siRNA was efficiently delivered into the cells even in the presence of phenamil in the delivery vehicle. As expected, noggin expression was similar and at normal level without noggin siRNA in the blank and SA/Chol/Phe groups. Phenamil is known to promote BMP activity through inducing Trb3.[16] Consistent results were observed with Trb3 staining for SA/Chol/Phe and SA/Chol/Phe+nogRNA groups. Trb3 was minimally expressed in the absence of phenamil. We also stained the late osteogenic marker OCN. The results showed intense staining for all the experimental groups treated with nanocarriers. Particularly, the combination delivery group showed highly intense OCN staining compared to the groups treated with phenamil or noggin siRNA alone.

We believe that cationic Sterosome formulated with SA/Chol is a safe, efficient and cost-effective nanocarrier to simultaneously deliver hydrophobic small molecular drug phenamil and noggin siRNA to mesenchymal stem cells. Encapsulation of phenamil provides a few advantages: no need to use organic solvent (e.g. DMSO) to solubilize those hydrophobic molecules; significantly reduction of drug dosage to achieve similar bioactivity; sustained and controlled release. Both *in vitro* and *in vivo* results confirmed that co-delivery of phenamil and noggin siRNA can benefit from the synergistic effects, since they enhance osteogenesis through different mechanisms. Shah and co-workers reported co-delivery of siRNA and hydrophobic small molecules with cyclodextrin-modified dendritic polyamine construct to neural stem cells to enhance differentiation into neurons.[42] Another co-delivery system of nucleic acids and small molecular drugs, self-assembled from phenylboronic acid modified oligoethylenimine and 1,3-diol-rich hyperbranched polyglycerol, was reported.[43, 44] Compared to the co-delivery systems reported in the literature, our SA/Chol Sterosomes showed promising advantages: (1) our delivery vehicles made from mixture of stearylamine and cholesterol; both components are small molecules, which are much easier to obtain and purify compared to macromolecules (e.g. polymers); (2) one of the components cholesterol was reported to enhance osteoblastic differentiation,[45] giving its intrinsic bioactive; (3) it would be easy for our system to scale up to meet the industry requirements. One predictable feature of our Sterosomes is the expandability of

function diversity by introducing other functional components *via* surface modification, which has already been thoroughly studied on traditional phospholipid liposomes.[2, 46]

4. Conclusion

The present study showed the ability of the new Sterosomes consisting of equimolar monoalkylated primary amine (SA) and Chol to efficiently and simultaneously deliver small molecular drug phenamil and noggin siRNA to direct MSC osteogenesis. SA/Chol Sterosomes supported sustained release of phenamil and demonstrated osteogenic efficacy at significantly reduced phenamil dosage compared with free phenamil. Furthermore, simultaneous delivery of noggin siRNA in the Sterosomes synergistically enhanced MSC osteogenesis *in vitro* and bone formation *in vivo* induced by phenamil. By manipulating the levels of BMP signaling antagonists and agonists, this co-delivery system will provide more sophisticated therapeutic strategies of maximal bone regeneration. Our findings suggest a simple and effective approach to co-delivering therapeutic genes and small molecular drugs using Sterosomes for combined therapy.

Supplementary Material

Refer to Web version on PubMed Central for supplementary material.

Acknowledgments

This work was supported by the National Institutes of Health [grant numbers R01 AR060213, R21 DE021819].

References

1. Bangham AD, Horne RW. Negative staining of phospholipids and their structural modification by surface-active agents as observed in the electron microscope. J Mol Biol. 1964; 8:660–8. [PubMed: 14187392]
2. Torchilin VP. Recent advances with liposomes as pharmaceutical carriers. Nat Rev Drug Discovery. 2005; 4:145–60. [PubMed: 15688077]
3. Blanco E, Hsiao A, Mann AP, Landry MG, Meric-Bernstam F, Ferrari M. Nanomedicine in cancer therapy: Innovative trends and prospects. Cancer Sci. 2011; 102:1247–52. [PubMed: 21447010]
4. Mitragotri S. Synergistic effect of enhancers for transdermal drug delivery. Pharm Res. 2000; 17:1354–9. [PubMed: 11205727]
5. Walsh C. Molecular mechanisms that confer antibacterial drug resistance. Nature. 2000; 406:775–81. [PubMed: 10963607]
6. Xu Y, Szoka FC. Mechanism of DNA release from cationic liposome/DNA complexes used in cell transfection. Biochemistry. 1996; 35:5616–23. [PubMed: 8639519]
7. Zelphati O, Szoka FC. Intracellular distribution and mechanism of delivery of oligonucleotides mediated by cationic lipids. Pharm Res. 1996; 13:1367–72. [PubMed: 8893276]
8. Hong K, Zheng W, Baker A, Papahadjopoulos D. Stabilization of cationic liposome-plasmid DNA complexes by polyamines and poly(ethylene glycol)-phospholipid conjugates for efficient in vivo gene delivery. FEBS Lett. 1997; 400:233–7. [PubMed: 9001404]
9. Cui ZK, Lafleur M. Lamellar self-assemblies of single-chain amphiphiles and sterols and their derived liposomes: Distinct compositions and distinct properties. Colloid Surface B. 2014; 114:177–85.
10. Ma JL, Both SK, Yang F, Cui FZ, Pan JL, Meijer G, Jansen JA, van den Beucken J. Concise review: Cell-based strategies in bone tissue engineering and regenerative medicine. Stem Cells Transl Med. 2014; 3:98–107. [PubMed: 24300556]

11. Mizuno H, Tobita M, Uysal AC. Concise review: Adipose-derived stem cells as a novel tool for future regenerative medicine. Stem Cells. 2012; 30:804–10. [PubMed: 22415904]
12. Peterson B, Zhang J, Iglesias R, Kabo M, Hedrick M, Benhaim P, Lieberman JR. Healing of critically sized femoral defects, using genetically modified mesenchymal stem cells from human adipose tissue. Tissue Eng. 2005; 11:120–9. [PubMed: 15738667]
13. Cahill KS, Chi JH, Day A, Claus EB. Prevalence, complications, and hospital charges associated with use of bone-morphogenetic proteins in spinal fusion procedures. JAMA-J Am Med Assoc. 2009; 302:58–66.
14. Epstein NE. Pros, cons, and costs of INFUSE in spinal surgery. Surg neurol int. 2011; 2:10–4. [PubMed: 21297932]
15. Smucker JD, Rhee JM, Singh K, Yoon ST, Heller JG. Increased swelling complications associated with off-label usage of rhBMP-2 in the anterior cervical spine. Spine. 2006; 31:2813–9. [PubMed: 17108835]
16. Park KW, Waki H, Kim WK, Davies BSJ, Young SG, Parhami F, Tontonoz P. The small molecule phenamil induces osteoblast differentiation and mineralization. Mol Cell Biol. 2009; 29:3905–14. [PubMed: 19433444]
17. Fan JB, Im CS, Cui ZK, Guo M, Bezouglaia O, Fartash A, Lee JY, Nguyen J, Wu BM, Aghaloo T, Lee M. Delivery of phenamil enhances BMP-2-induced osteogenic differentiation of adipose-derived stem cells and bone formation in calvarial defects. Tissue Eng Part A. 2015; 21:2053–65. [PubMed: 25869476]
18. Pal R, Mamidi MK, Das AK, Bhonde R. Diverse effects of dimethyl sulfoxide (DMSO) on the differentiation potential of human embryonic stem cells. Arch Toxicol. 2012; 86:651–61. [PubMed: 22105179]
19. Jorgensen WL, Duffy EM. Prediction of drug solubility from structure. Adv Drug Deliv Rev. 2002; 54:355–66. [PubMed: 11922952]
20. Wan DC, Pomerantz JH, Brunet LJ, Kim JB, Chou YF, Wu BM, Harland R, Blau HM, Longaker MT. Noggin suppression enhances in vitro osteogenesis and accelerates in vivo bone formation. J Biol Chem. 2007; 282:26450–9. [PubMed: 17609215]
21. Gazzerro E, Gangji V, Canalis E. Bone morphogenetic proteins induce the expression of noggin, which limits their activity in cultured rat osteoblasts. J Clin Investig. 1998; 102:2106–14. [PubMed: 9854046]
22. Gazzerro E, Du Z, Devlin RD, Rydziel S, Priest L, Economides A, Canalis E. Noggin arrests stromal cell differentiation in vitro. Bone. 2003; 32:111–9. [PubMed: 12633782]
23. Fan JB, Park H, Tan S, Lee M. Enhanced osteogenesis of adipose derived stem cells with noggin suppression and delivery of BMP-2. PLoS One. 2013:8.
24. Cui ZK, Fan J, Kim S, Bezouglaia O, Fartash A, Wu BM, Aghaloo T, Lee M. Delivery of siRNA via cationic Sterosomes to enhance osteogenic differentiation of mesenchymal stem cells. J Control Release. 2015; 217:42–52. [PubMed: 26302903]
25. Fan J, Park H, Lee M, Bezouglaia O, Kim J, Aghaloo T, Lee M. Adipose derived stem cells and BMP-2 delivery in chitosan-based 3D constructs to enhance bone regeneration in a rat mandibular defect model. Tissue Eng Part A. 2014; 20:2169–79. [PubMed: 24524819]
26. Cui ZK, Bouisse A, Cottenye N, Lafleur M. Formation of pH-sensitive cationic liposomes from a binary mixture of monoalkylated primary amine and cholesterol. Langmuir. 2012; 28:13668–74. [PubMed: 22931455]
27. Carbajal G, Cui ZK, Lafleur M. Non-phospholipid liposomes with high sterol content display a very limited permeability. Sci China-Chem. 2013; 56:40–7.
28. Estes BT, Diekman BO, Gimble JM, Guilak F. Isolation of adipose-derived stem cells and their induction to a chondrogenic phenotype. Nat Protoc. 2010; 5:1294–311. [PubMed: 20595958]
29. Hu J, Hou Y, Park H, Choi B, Hou S, Chung A, Lee M. Visible light crosslinkable chitosan hydrogels for tissue engineering. Acta Biomater. 2012; 8:1730–8. [PubMed: 22330279]
30. Gregory CA, Gunn WG, Peister A, Prockop DJ. An Alizarin red-based assay of mineralization by adherent cells in culture: comparison with cetylpyridinium chloride extraction. Anal Biochem. 2004; 329:77–84. [PubMed: 15136169]

31. Muller RH, Jacobs C, Kayser O. Nanosuspensions as particulate drug formulations in therapy rationale for development and what we can expect for the future. Adv Drug Deliv Rev. 2001; 47:3–19. [PubMed: 11251242]
32. Cui ZK, Lafleur M. Lamellar self-assemblies of single-chain amphiphiles and sterols and their derived liposomes: Distinct compositions and distinct properties. Colloid Surf B- Biointerfaces. 2014; 114:177–85. [PubMed: 24184913]
33. Campbell PI. Toxicity of some charged lipids used in liposome preparations. Cytobios. 1983; 37:21–6. [PubMed: 6851664]
34. Dokka S, Toledo D, Shi XG, Castranova V, Rojanasakul Y. Oxygen radical-mediated pulmonary toxicity induced by some cationic liposomes. Pharm Res. 2000; 17:521–5. [PubMed: 10888302]
35. Romoren K, Thu BJ, Bols NC, Evensen O. Transfection efficiency and cytotoxicity of cationic liposomes in salmonid cell lines of hepatocyte and macrophage origin. Biochim Biophys Acta-Biomembr. 2004; 1663:127–34.
36. Nguyen MK, Lee DS. Injectable biodegradable hydrogels. Macromol Biosci. 2010; 10:563–79. [PubMed: 20196065]
37. Slaughter BV, Khurshid SS, Fisher OZ, Khademhosseini A, Peppas NA. Hydrogels in regenerative medicine. Adv Mater. 2009; 21:3307–29. [PubMed: 20882499]
38. Park H, Choi B, Hu J, Lee M. Injectable chitosan hyaluronic acid hydrogels for cartilage tissue engineering. Acta Biomater. 2013; 9:4779–86. [PubMed: 22935326]
39. Arakawa C, Ng R, Tan S, Kim S, Wu B, Lee M. Photopolymerizable chitosan-collagen hydrogels for bone tissue engineering. J Tissue Eng Regen Med. 2014; doi: 10.1002/term.896
40. Choi B, Kim S, Fan JB, Kowalski T, Petrigliano F, Evseenko D, Lee M. Covalently conjugated transforming growth factor-beta 1 in modular chitosan hydrogels for the effective treatment of articular cartilage defects. Biomater Sci. 2015; 3:742–52. [PubMed: 26222593]
41. Choi B, Kim S, Lin B, Li K, Bezouglaia O, Kim J, Evseenko D, Aghaloo T, Lee M. Visible-light-initiated hydrogels preserving cartilage extracellular signaling for inducing chondrogenesis of mesenchymal stem cells. Acta Biomater. 2015; 12:30–41. [PubMed: 25462526]
42. Shah S, Solanki A, Sasmal PK, Lee KB. Single vehicular delivery of siRNA and small molecules to control stem cell differentiation. J Am Chem Soc. 2013; 135:15682–5. [PubMed: 24106916]
43. Jia HZ, Zhang W, Wang XL, Yang B, Chen WH, Chen S, Chen G, Zhao YF, Zhuo RX, Feng J, Zhang XZ. Polymeric assembly of hyperbranched building blocks to establish tunable nanoplatforms for lysosome acidity-responsive gene/drug co-delivery. Biomater Sci. 2015; 3:1066–77. [PubMed: 26221940]
44. Jia HZ, Zhang W, Zhu JY, Yang B, Chen S, Chen G, Zhao YF, Feng J, Zhang XZ. Hyperbranched-hyperbranched polymeric nanoassembly to mediate controllable co-delivery of siRNA and drug for synergistic tumor therapy. J Control Release. 2015; 216:9–17. [PubMed: 26272764]
45. Li HF, Guo HJ, Li H. Cholesterol loading affects osteoblastic differentiation in mouse mesenchymal stem cells. Steroids. 2013; 78:426–33. [PubMed: 23395977]
46. Sawant RR, Torchilin VP. Liposomes as ‘smart’ pharmaceutical nanocarriers. Soft Matter. 2010; 6:4026–44.

Statement of Significance

Application of phenamil, a small molecular bone morphogenetic protein (BMP) stimulator, combined with suppression of natural BMP antagonists such as noggin is a promising therapeutic strategy to enhance bone regeneration. Here, we present a novel strategy to co-deliver hydrophobic small molecule phenamil and noggin-targeted siRNA *via* cationic Sterosomes formed with Stearylamine (SA) and high content of Cholesterol (Chol) to enhance osteogenesis and bone repair. SA/Chol Sterosomes demonstrated high phenamil encapsulation efficiency, supported sustained release of encapsulated drugs, and significantly reduced drug dose requirements to induce osteogenic differentiation of mesenchymal stem cells (MSCs). Simultaneous deliver of phenamil and noggin siRNA in a single vehicle synergistically enhanced MSC osteogenesis and calvarial bone repair. This study suggests a new non-phospholipid liposomal formulation to simultaneously deliver small molecules and therapeutic genes for combined treatment.

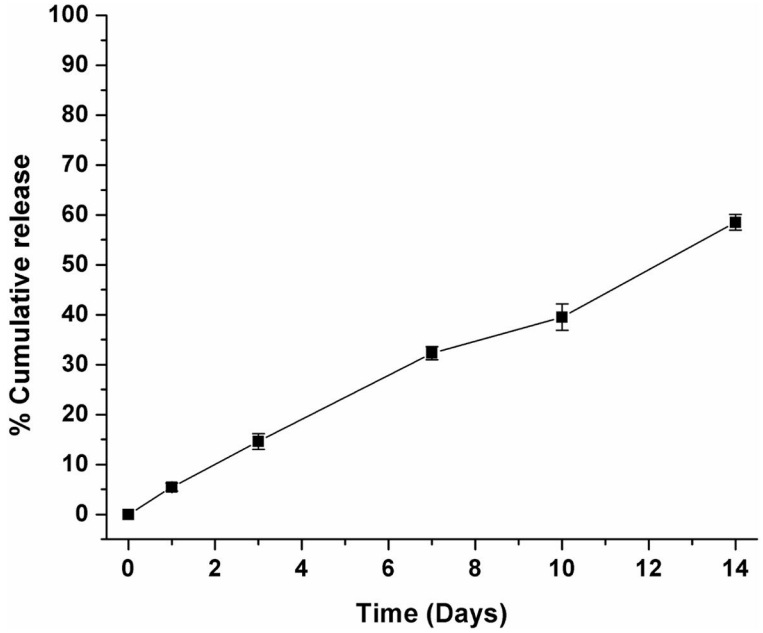

Figure 1.
Release profile of phenamil encapsulated in SA/Chol liposomes, at 25 °C pH 7.4. (n = 3)

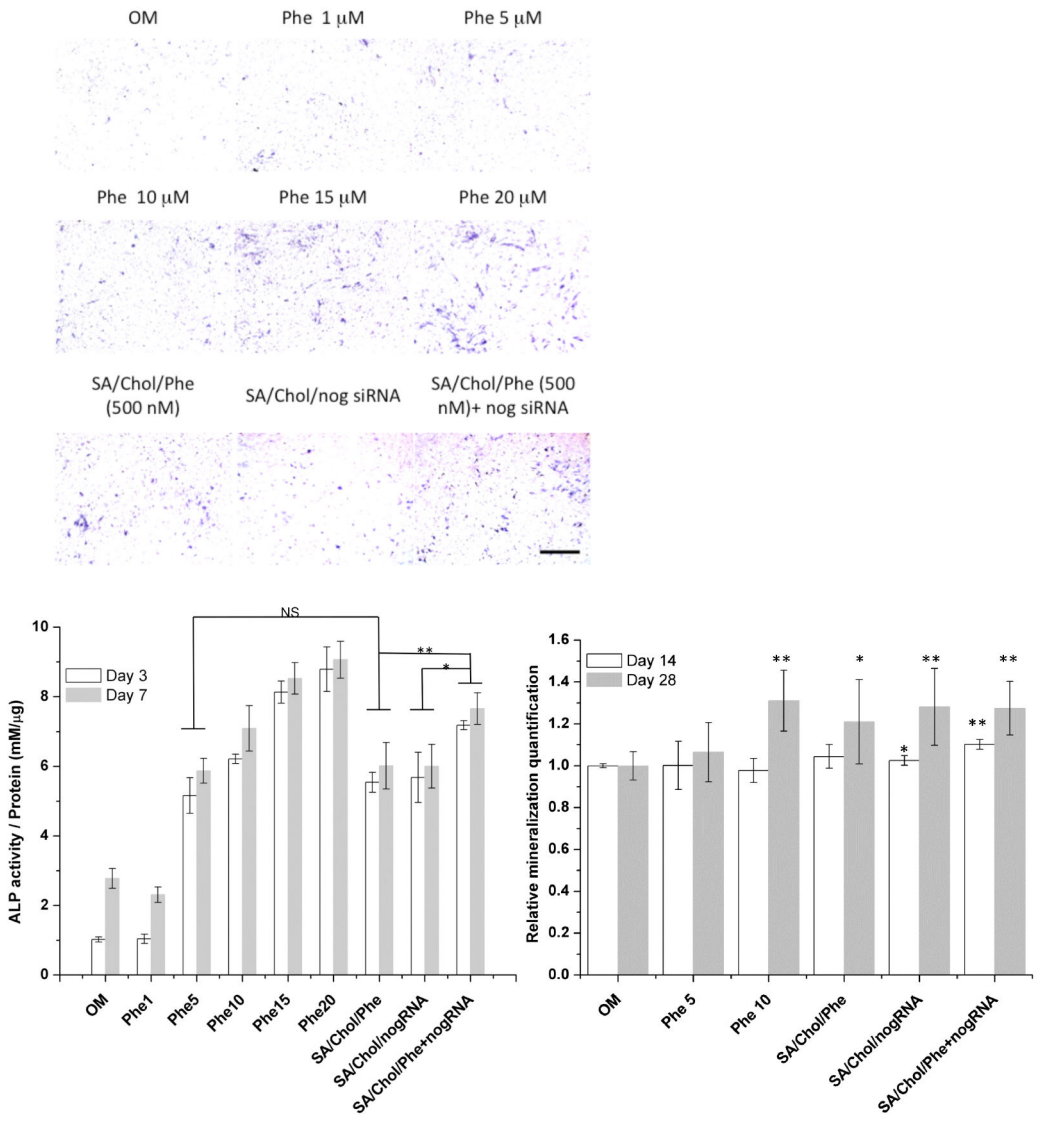

Figure 2.

Alkaline phosphatase (ALP) expression of MSCs in 2D monolayer cell culture on day 7 (A), scale bar 500 μm. Colorimetric quantification of ALP activity (B) on day 3 (white) and 7 (grey), (n = 4, *p < 0.05, **p < 0.001, NS = no significance).

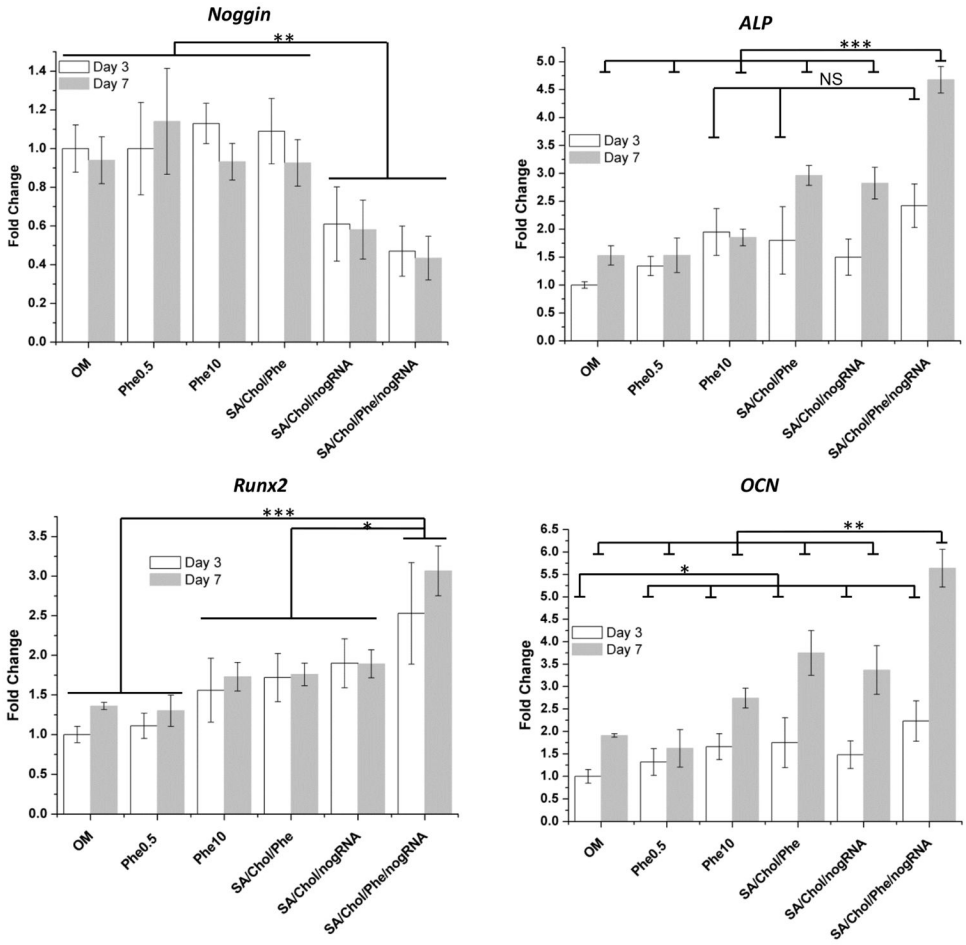

Figure 3.

Various gene expression of MSCs in 2D monolayer cell culture. Gene markers including *Noggin, ALP, Runx2*, and *OCN* were evaluated on day 3 (white) and 7 (grey), (n = 5, *p < 0.05, **p < 0.01, ***p < 0.001 and NS = no significance).

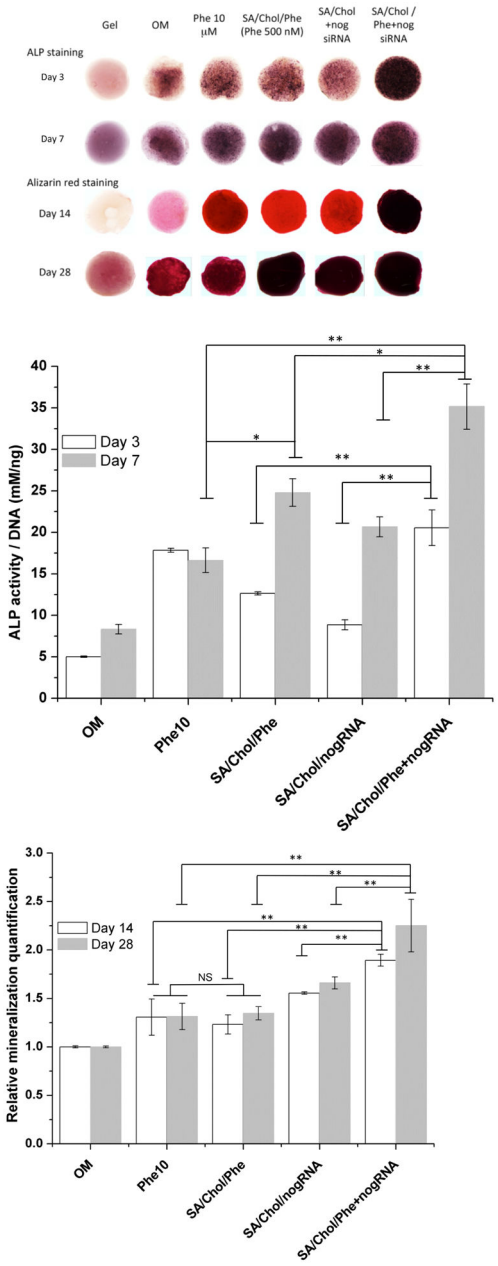

Figure 4.

Alkaline phosphatase (ALP) expression and mineralization of MSCs stained with Alizarin red S in hydrogels (A); Colorimetric quantification of ALP activity (B) on day 3 (white) and 7 (grey); and mineralization (C) on day 14 (white) and 28 (grey), (n = 4, *p < 0.05, **p < 0.001, NS = no significance).

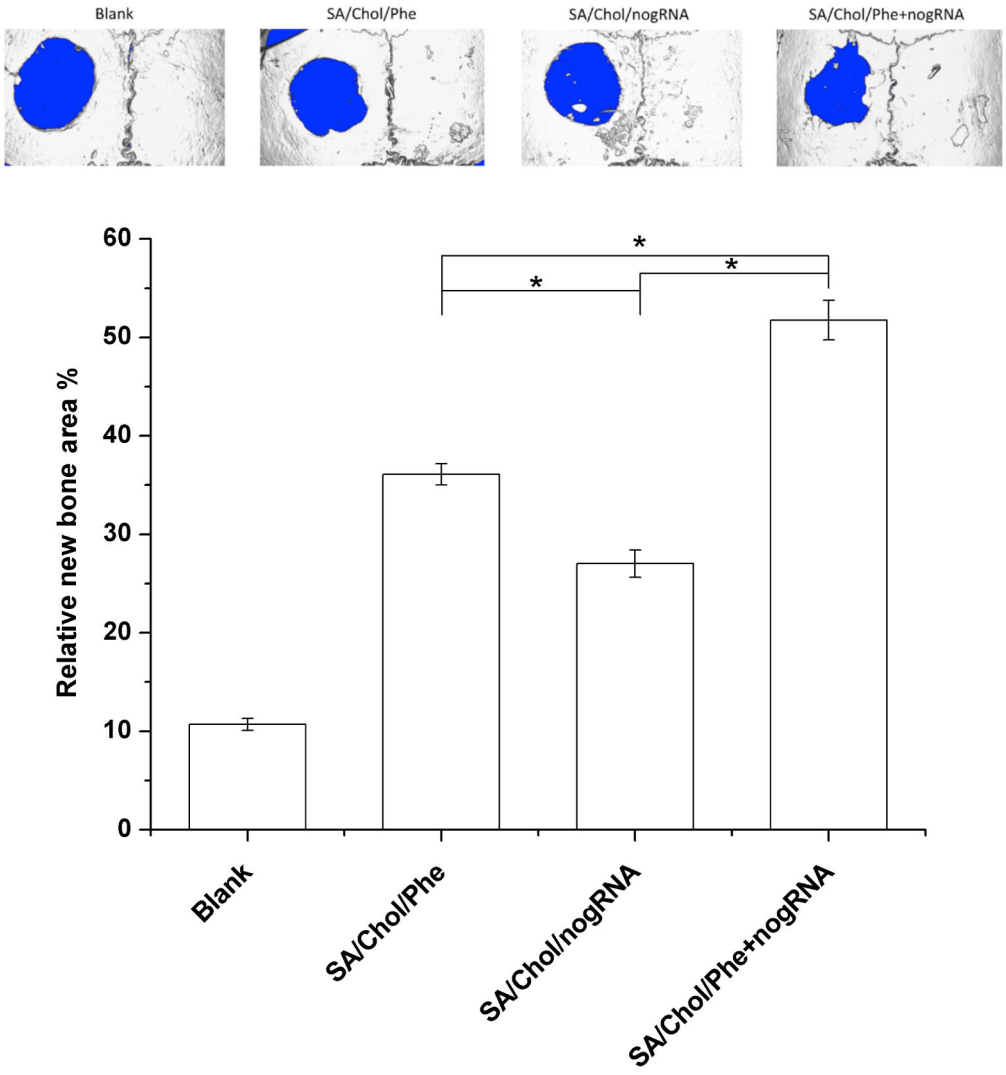

Figure 5.

(A) Micro-computed tomography images of calvarial defects treated with/without MeGC hydrogels encapsulated with MSCs and nanoparticles. (B) Quantification of relative new bone area in calvarial defects. (*$p < 0.05$)

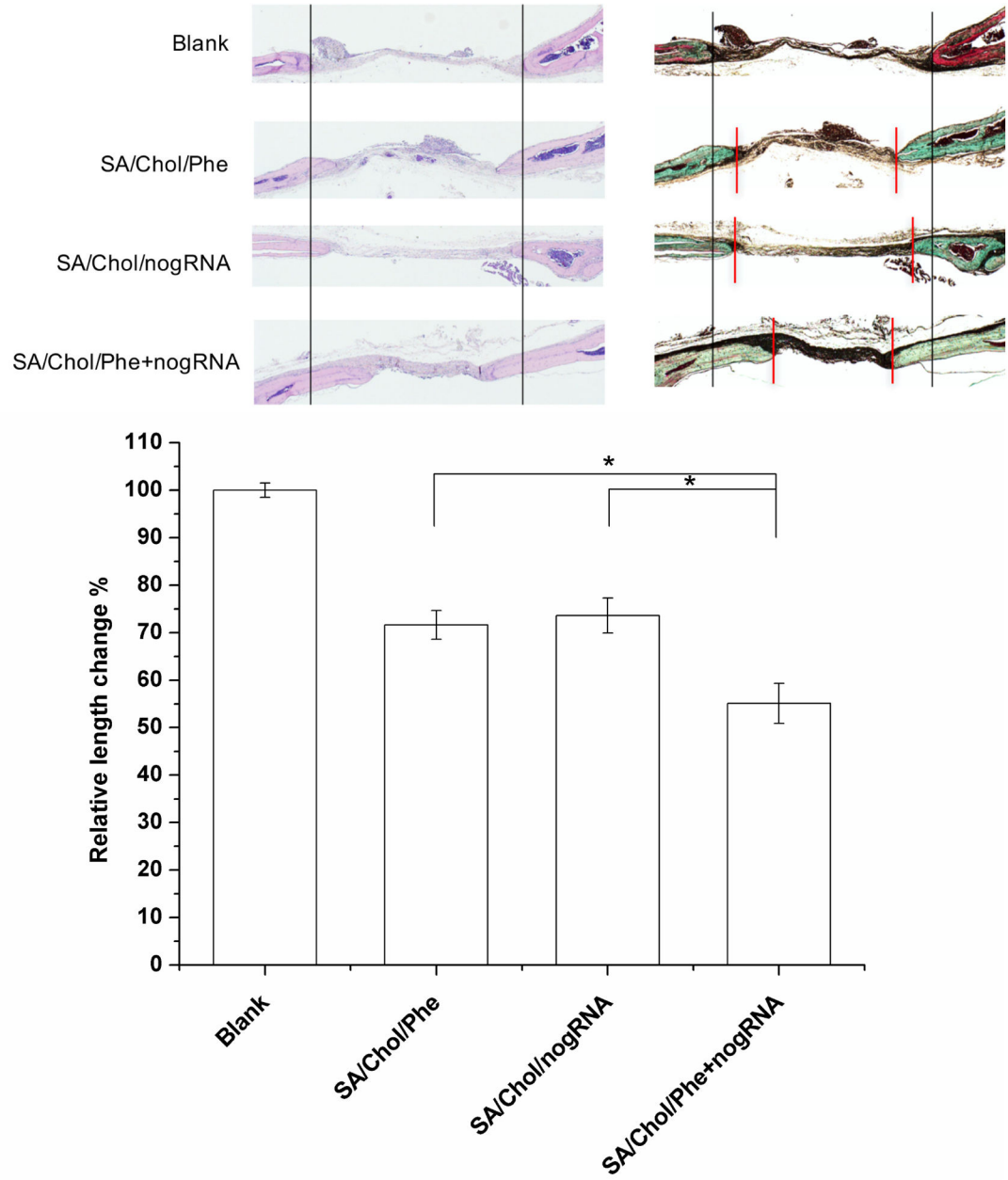

Figure 6.

Histological analysis of bone regeneration in calvarial defects. (A) Hematoxylin-eosin staining (Left), Masson-Goldner trichrome staining (Right). Two black vertical lines were drawn for the ease of observation. (B) The relative length change was measured and normalized to the blank group. Red vertical lines indicate the edges of the advancing bone. (n = 4)

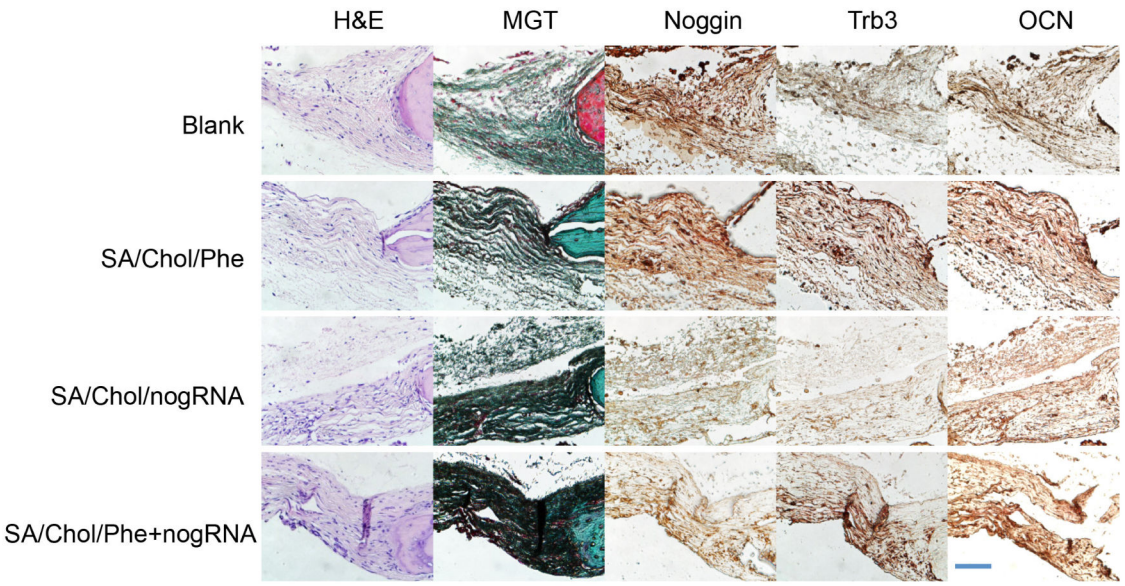

Figure 7.

Magnified images of H&E and Masson-Goldner trichrome staining. Immunohistochemical staining of noggin, Trb3 and OCN. Scale bar = 50 μm.